Journal of Polymer Science and Engineering 2026, 9(1), 026100004.
https://doi.org/10.24294/jpse026100004

Article

Synthesized TiO_2 nanoparticles mitigating salinity stress in okra plants via foliar application

Mehmood Khan[1], Bilal Ahmad[1], Ikram Ullah[1], Muhammad Ayub Khan[2], Sara Begum[1], Sara Bibi[1], Attaullah Khan[1], Mohsin Ali[1], Shahab Khan[3,*], Noor Ul Islam[1,*]

[1] Department of Chemistry, Government Degree College Lalqilla Dir Lower, Lalqilla 18350, Khyber Pakhtunkhwa, Pakistan
[2] Department of Chemistry, Ghazi Umara Khan Degree College Samar Bagh Dir Lower, Samar Bagh 18600, Khyber Pakhtunkhwa, Pakistan
[3] Department of Chemistry, University of Malakand, Chakdara 18800, Khyber Pakhtunkhwa, Pakistan.
*** Corresponding authors:** Shahab Khan, shahabkhan262@gmail.com; Noor Ul Islam, nooruomchem@gmail.com

CITATION

Khan M, Ahmad B, Ullah I, et al. Synthesized TiO2 nanoparticles mitigating salinity stress in okra plants via foliar application. Journal of Polymer Science and Engineering. 2026; 9(1): 026100004. https://doi.org/10.24294/jpse026100004

ARTICLE INFO

Received: 8 March 2026
Accepted: 11 June 2026
Available online: 30 June 2026

Abstract: Titanium dioxide nanoparticles (TiO_2 NPs) are increasingly recognized for their potential to enhance plant growth under abiotic stress conditions. In this study, TiO_2 NPs were synthesized via a modified sol–gel method. The successful formation of anatase TiO_2-NPs with uniformly quasi-spherical morphology was confirmed using multiple characterization techniques, including X-ray diffraction, field emission scanning electron microscopy, energy-dispersive X-ray spectroscopy, and Raman spectroscopy. Furthermore, we investigated the effects of foliar application of prepared TiO_2 NPs at 100 and 150 ppm on okra (Abelmoschus esculentus) grown under salt stress (100 ppm NaCl). The target variables evaluated included plant height, number of leaves, fresh and dry biomass, chlorophyll a, chlorophyll b, total chlorophyll, carotenoids, sugar content, and proline accumulation to determine the role of TiO_2 NPs in salt stress mitigation. Salinity negatively affected all measured agronomic and physiological traits; however, treatment with TiO_2 NPs mitigated these adverse effects. Treated plants exhibited improved plant growth and yield-related characteristics, alongside higher concentrations of chlorophyll a, chlorophyll b, total chlorophyll, and carotenoids. Among the tested concentrations, 150 ppm TiO_2 NPs showed the most pronounced improvement in growth, photosynthetic pigments, and yield performance under saline conditions. These findings indicate that foliar application of TiO_2 NPs, particularly at 150 ppm, may play an important role in alleviating the detrimental effects of salinity stress on okra. Statistical analysis was performed using two-way ANOVA to assess the effects of variety, treatment, and their interaction, followed by Tukey's HSD test for mean separation at $p \leq 0.05$ using IBM SPSS Statistics.

Keywords: TiO_2 nanoparticle; salinity stress; foliar spray; nano-fertilizer; croft quality and yield

1. Introduction

Titanium dioxide nanoparticles (TiO_2 NPs) are among the most widely studied nanomaterials globally. They are considered environmentally friendly because of their stability, relatively low toxicity, and photocatalytic activity [1]. These characteristics of TiO_2 NPs have attracted significant consideration in agriculture, in particular, for improving plant growth and tolerance against abiotic stresses such as salinity. Because of its high surface-to-volume ratio, anatase TiO_2 -NPs are the most stable and reactive phase [2]. Modern-day synthesis techniques, including sol–gel, hydrothermal, solvothermal, and co-precipitation methods, enable precise control over particle size, shape, and crystallinity to enhance performance [3].

In the field of agriculture, TiO_2-NPs are considered multifunctional agents to improve crop growth, yield, and resistance against salinity. A literature study indicates that they can enhance photosynthesis, improve nitrogen metabolism, promote seed germination, and increase chlorophyll and protein content in various crops such as spinach, rice, sunflower, maize, and coriander [4]. In addition, TiO_2-NPs have been reported to increase the antioxidant defense system and regulate reactive oxygen species (ROS) production. Therefore, they reduce oxidative damage in crops under salinity stress conditions. While enhancing biomass and crop productivity, the antibacterial properties of TiO_2-NPs contribute to reducing plant disease [5]. Additionally, TiO_2-NPs can mitigate numerous environmental stresses, such as salinity, drought, and heavy metal contamination, by strengthening antioxidant defense and regulating ROS [6]. However, their mitigating effects are strongly concentration-dependent. For example, at low to moderate doses (2–300 mgL^{-1}), TiO_2-NPs generally promote plant growth and yield. In contrast, they may inhibit photosynthesis and induce oxidative stress at higher concentrations (>1000 mgL^{-1}) [7]. Interestingly, such stress may also trigger beneficial antioxidant responses that strengthen the plant defense system [8].

Among several abiotic stresses, soil salinity is counted as one of the severest constraints affecting agricultural productivity globally, particularly in arid and semi-arid areas [9]. Salinity stress badly affects plant growth by escalating osmotic pressure, limiting water uptake, and interrupting nutrient balance [10]. These adverse effects lead to ROS, ion toxicity, membrane damage, metabolic disturbances, and eventually reduced crop yield [11,12]. Globally, about 23% of cultivated land is saline, while approximately 37% is sodic [13,14]. Salinity may develop naturally via long-term environmental processes or be enhanced by anthropogenic activities such as poor drainage and improper irrigation [14]. To live longer under saline conditions, plants adopt various adaptive mechanisms such as salt elimination, intracellular ion compartmentalization, osmotic tuning, and activation of antioxidant defense systems [11,13,15,16]. Nevertheless, continued exposure to salinity brutally spoils physiological and biochemical processes, by this means restraining plant productivity.

Okra (*Abelmoschus esculentus*) is an important vegetable crop in subtropical regions, not only as a vegetable but also for its wide range of uses. Its seeds are used to produce oil, protein, and even coffee substitutes. Additionally, its leaves and stems can be processed into biomass, paper, or fuel. With a nutritional value index of 3.21, okra holds high nutritional value and is cultivated across Asia, Africa, and the Americas [17,18]. Despite its nutritional value, okra growth and productivity are highly sensitive to salinity stress, which drastically reduces its agronomic performance. TiO_2-NPs have been explored in numerous crops; however, studies concerning their effects on okra are very limited. Additionally, the potential of TiO_2-NPs to alleviate salinity-induced stress in okra under saline conditions via foliar application has not been sufficiently explored, particularly in relation to agronomic and physiological responses.

Due to the significant role of TiO_2-NPs in sustainable agriculture, this study aimed to explore the potential of TiO_2-NPs to improve okra growth under salt stress conditions through foliar application. In this regard, TiO_2-NPs was synthesized via a sol-gel method and characterized by various techniques, such as X-ray Diffraction

(XRD), Scanning Electron Microscopy (SEM), Energy Dispersive X-ray (EDX), photoluminescence, and Raman spectroscopy. Aqueous solutions (100 and 150 ppm) of as-prepared TiO_2-NPs were applied as foliarly to two okra varieties: Sabaz Pari (V1) and Savanta (V2), grown under 100 mM saline stress. Agronomic and physiological parameters were assessed to determine the usefulness of TiO_2-NPs in mitigating salinity stress in okra.

2. Materials and methods

2.1. Preparation of TiO_2-NPs

TiO_2-NPs were synthesized using the sol–gel method. Briefly, 8.4 mL of titanium isopropoxide was mixed with 24 mL of isopropanol under continuous stirring for 10 min. A solution of 2 mL of distilled water and 1 mL of isopropanol was then added dropwise, and the mixture was stirred for 24 h to form a gel. The gel was oven-dried at 100 ℃ in an oven, calcined in a furnace at 500 ℃ for 2 h at a heating rate of 5 ℃/min, finely ground, and stored for further use.

2.2. Characterization of the TiO_2-NPs

The as-prepared TiO_2-NPs were characterized using various techniques to elucidate their morphological, structural, and compositional properties. The surface morphology and microstructural features of the prepared TiO_2-NPs were examined by field-emission scanning electron microscopy (FESEM, Magellan 400, FEI, USA). Energy-dispersive X-ray spectroscopy (EDX) was used to investigate the elemental composition of TiO_2-NPs. The crystalline phase structures of the TiO_2 sample were determined using X-ray diffraction (XRD, Rigaku D/MAX 2500 V diffractometer) with Cu Kα radiation operated at 40 kV. Raman spectroscopy (LabRAM HR Evolution, Horiba Scientific, France) was performed at room temperature to further analyze the vibrational modes, phase purity, and structure of as-synthesized TiO_2-NPs.

2.3. Experimental layout

To examine the usefulness of as-prepared TiO_2-NPs in salt stress mitigation, the experiments were carried out during the cropping season of 2024 in Lalqilla, Dir Lower, Pakistan (34.66925 ° N, 72.06124 ° E; 2349 ft elevation). Two native okra varieties, Sabaz Pari (V1) and Savanta (V2), were obtained from the Agricultural Institute in Tarnab, Peshawar, Pakistan. Before sowing, seeds were surface sterilized with 50% ethanol, followed by 5% sodium hypochlorite, and then rinsed three times with distilled water to ensure purity. The sterilized seeds were then sown in soil and kept under open-field conditions throughout the study. During the entire experimental period, the average ambient temperature ranged from 24–30 ℃, relative humidity ranged from 60–70%, and plants were exposed to a natural photoperiod of approximately 12 h light/12 h dark cycle with average sunlight intensity of approximately 400–500 μmol m^{-2} s^{-1}. The soil used for this experiment was the naturally existing field soil of the experimental site in Lalqilla Dir Lower, Pakistan. The soil possessed a sandy loam texture with a pH of 7.5 and electrical conductivity (EC) of 1.1 dS m^{-1}. The soil was first air-dried, sieved, and homogenized to ensure

uniform physicochemical properties throughout the experiment, and then the seeds of the selected okra varieties were sown.

A Completely Randomized Block Design (CRBD) with three replications per treatment was employed, as shown in the **Table 1**.

Table 1. Experimental setup for evaluating the salinity-mitigating effect of TiO_2-NPs foliar spray on okra plants.

Symbolic representation	Treatments	Number of experiments
T0	Controle	3 times
T1	Saline (100 mM solution)	3 times
T2	Saline stress (100 mM NaCl solution) and TiO_2-NPs foliar spry (100 mgL^{-1} solution)	3 times
T3	Saline stress (100 mM NaCl solution) and TiO_2-NPs foliar spry (150 mgL^{-1} solution)	3 times

All plants were maintained under uniform conditions. Control plants (T0) were irrigated daily with distilled water, whereas plants in treatments T1–T3 were subjected to saline stress (100 mM NaCl). The synthesized TiO_2-NPs were dispersed in distilled water and stirred at high speed for 30 min to obtain a stable suspension before spraying. The TiO_2-NPs suspensions (100 and 150 ppm) were applied to T2 and T3 plants, respectively, by a hand-held atomizer sprayer at three-day intervals. Approximately 15–20 mL suspension per plant was applied consistently onto the leaf surfaces until near overflow. The data were analyzed using IBM SPSS Statistics software. A two-way analysis of variance (ANOVA) was performed to evaluate the effects of variety, treatment, and their interaction on sugar content, chlorophyll a (ChlA), chlorophyll b (ChlB), carotenoids (Carot), total chlorophyll (TChl), and proline. When significant differences were detected, treatment means were separated using Tukey's Honestly Significant Difference (HSD) test at the 5% probability level ($p \leq 0.05$). Results are presented as mean values, and treatments sharing different letters were considered significantly different.

2.4. Agronomic traits

Morphological parameters, including fresh and dry biomass, root length, and shoot length, were recorded. Leaf Area Ratio (LAR) was calculated using Equation 1.

$$LAR = \frac{leaf\ area\ (cm^2)}{final\ dry\ weight} \quad \textbf{(1)}$$

2.5. Physio-biochemical analyses

2.5.1. Sugar estimation

Fresh leaves (0.5 g) were homogenized in 10 mL of distilled water using a mortar and pestle, and centrifuged at 3000 rpm for 5 min. From the supernatant, 0.1 mL was taken and mixed with 1 mL of 80% phenol, followed by incubation at room temperature for 4 h. Subsequently, 5 mL concentrated H_2SO_4 was added, and absorbance was measured at 420 nm using a spectrophotometer. Total soluble sugar

content was estimated following the phenol–sulfuric acid method described by Dubois et al. [19].

Sugar concentration was calculated using Equation 2.

$$Sugar\ concetration\ (mgg^{-1}) = \frac{A \times K \times DF}{W} \quad (2)$$

Where *A* is the absorbance, *W* is the weight of the sample, *K* is a constant, and its value is 20, and *DF* is the dilution factor, and its value is 10.

2.5.2. Photosynthetic pigments

Photosynthetic pigments were determined by the 80% acetone extraction method [20]. Fresh leaf samples (0.5 g each) were homogenized in 10 mL of 80% acetone and kept in the dark at room temperature. After centrifugation (2000 rpm, 5 min), the supernatant was collected, and absorbance was recorded at 663, 645, and 470 nm against an 80% acetone blank. Pigment concentrations were calculated using Equations 3–5.

$$hlo\ "a"\ mgmL^{-1} = 12.7 \times A_{663} - 2.69 \times A_{645} \quad (3)$$

$$Chlo\ \text{"b"}\ mgmL^{-1} = 22.9 \times A_{645} - 4.68 \times A_{663} \quad (4)$$

$$Total\ Carotenoids\ mgL^{-1} = \frac{1000A_{470} - 2.27(Chlo\ a) - 81.4(Chlo\ b)}{198} \quad (5)$$

2.5.3. Proline estimation

Proline content was quantified following the method of Bates et al. (1973). Leaf tissue (0.5 g) was homogenized in 10 mL of 3% sulphosalicylic acid and filtered. 2 mL of the filtrate were mixed with the solution of 4 mL of glacial acetic acid and 4 mL of 20% ninhydrin. The mixture was then incubated at 100 ℃ for 1 h, cooled, and extracted with 4 mL toluene. Absorbance was measured at 520 nm, and proline concentration was calculated using Equation 6.

$$Proline\ content\ (\mu gg^{-1}) = \frac{A \times K \times DF}{W} \quad (6)$$

Where *A* is the absorbance of the sample, *W* is the weight of the sample, *K* is a constant and its value of 17.52, and *DF* is the dilution factor, and its value of 2.

3. Results

3.1. Characterization of TiO_2 NPs

To study the morphology of TiO_2 NPs, FE-SEM analysis was performed. The FE-SEM images (**Figure 1a**,**b**) exhibit that the prepared TiO_2-NPs show a relatively uniform, quasi-spherical morphology with slight agglomeration. The average particle size was quantified by measuring particles from a high-magnification FE-SEM image using image analysis software. The obtained histogram (**Figure 1c**) showed that maximum particles were dispersed within the range of 50–77 nm, thus, presenting a relatively narrow and homogenous size distribution. The average particle size was found to be 67.5 nm.

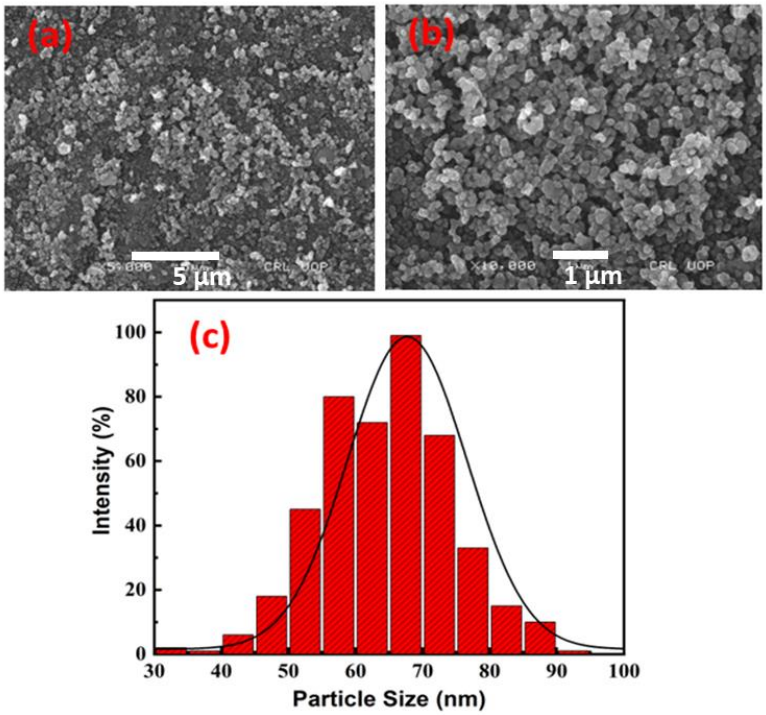

Figure 1. (**a**, **b**) Field Emission Scanning Electron Microscopic images of TiO_2-NPs, and (**c**) particle size distribution histogram of TiO_2-NPs.

EDX spectroscopic analysis was carried out to determine the elemental composition of the prepared TiO_2-NPs, and the corresponding EDX spectrum is presented in **Figure 2**. The results confirmed the presence of titanium (Ti) and oxygen (O) as the main constituent elements, consistent with the stoichiometry of TiO_2-NPs. In addition to these elements, a minor peak consistent with carbon was also observed.

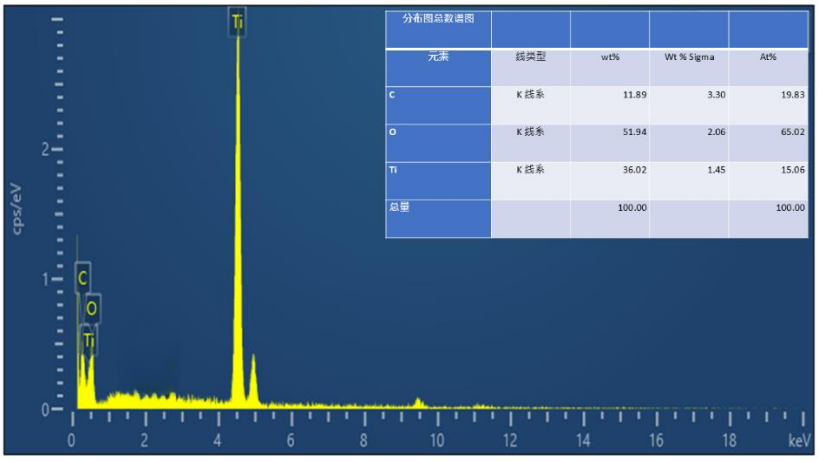

Figure 2. Energy Dispersive X-ray spectrum of as-prepared TiO2-NPs.

Figure 3a illustrates the XRD pattern of TiO_2 NPs. The diffraction peaks appear at 2θ values of 25.36°, 36.95°, 37.81°, 38.57°, 48.09°, 53.97°, 55.21°, 62.71°, 68.75°, 70.30 °, 75.10 °, and 82.68 °, can be indexed to the (101), (103), (004), (112), (200), (105), (211), (204), (116), (220), (215), and (224) planes, respectively. The average crystallite size of the as-prepared TiO_2-NPs was calculated using the Scherrer equation, and was typically found in the range of 15–25 nm.

Raman spectroscopy was utilized to evaluate the structural integrity and phase composition of TiO_2-NPs. As demonstrated in **Figure 3b**, the TiO_2-NPs shows four well-defined Raman active modes sited at ~144, ~398, ~518, and ~642 cm^{-1}. These bands are allotted to the E_g, B_{1g}, A_{1g}, and E_g vibrational modes, respectively. These bands are characteristic of the anatase phase of TiO_2 NPs.

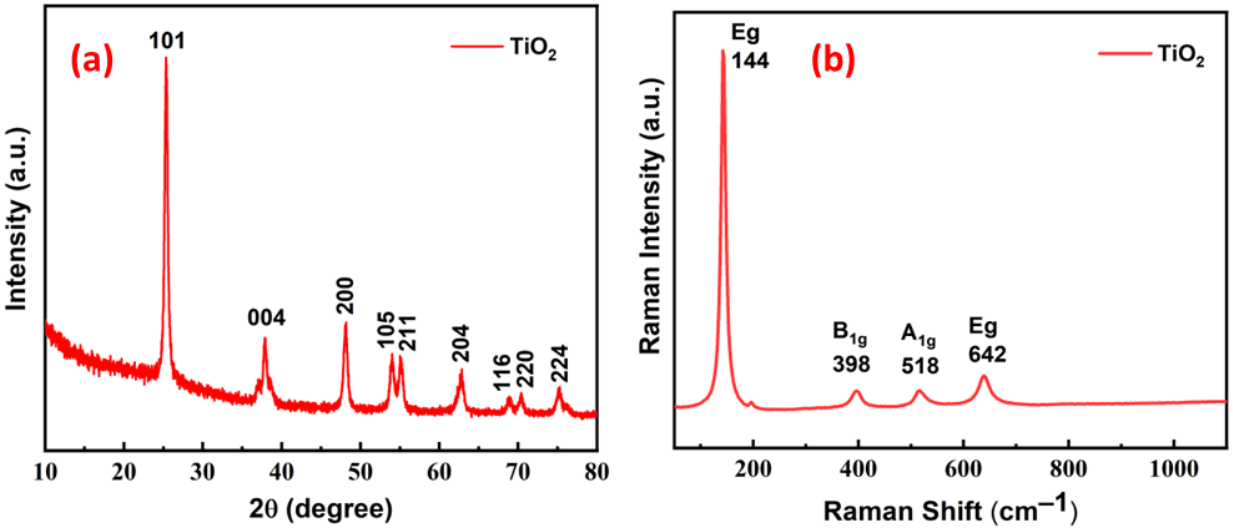

Figure 3. (**a**) X-ray Diffraction pattern and (**b**) Raman spectrum of TiO_2 nanoparticles.

3.2. Agronomic study of experimental plants

The growth performance of the two okra varieties is summarized in **Table 1**. Under saline stress (T1), plants exhibited marked reductions in root length, shoot length, leaf area, total weight, and dry weight compared with the control (T0). Application of TiO_2-NPs sprays (T2 and T3), however, enhanced plant growth, with values approaching or even exceeding those of the control. Notably, the 100 ppm TiO_2-NPs treatment yielded better results than the 150 ppm treatment. Overall, these findings indicate that TiO_2-NPs supports okra growth under salinity stress, although higher concentrations may exert adverse effects.

Table 1. Foliar application effects of TiO_2-NPs on the root and shoot length, leaf area, total weight and dry weight of the okra plant under induced saline stress.

Treatment	Root length (cm)		Shoot length (cm)		Leaf area (cm^2)		Total weight (g)		Dry weight (g)	
	V1	V2	V1	V2	V1	V2	V1	V2	V1	V2
T_0	15.95 ± 1.17	24.5 ± 0.50	41 ±0.33	44.66 ± 0.50	216.3 ±3.0	314 ± 1.88	33.32 ± 0.32	68.9 ±0.49	4.78 ± 0.10	8.67 ± 0.15
T1	13.5 ± 0.19	16 ±0.50	30 ±0.66	32.5 ±0.92	82.7 ±1.06	82.5 ± 1.17	6.72 ±0.13	30.4 ±1.13	0.91 ± 0.04	4.57 ± 0.01
T2	16.75 ± 0.09	22.5 ± 0.50	42.33 ± 0.62	58.66 ± 0.50	189.37 ± 2.06	328 ± 3.77	21.15 ± 0 .54	60.09 ± 0.89	3.33 ± 0.08	7.69 ± 0.05
T3	10.5 ±0.33	25.5 ± 0.50	41.83 ± 0.41	59.66 ± 0.50	112.5 ±0.70	115 ± 2.35	22.75 ± 0.11	22.7 ±3.91	2.50 ± 0.15	2.86 ± 0.01

3.3. Photosynthetic pigments

Photosynthetic pigments are a useful indicator of how plants respond to environmental stress, as changes in their levels often reflect reduced photosynthetic efficiency and visible stress symptoms. The photosynthetic pigments of the control and treated plants were measured and the results are displayed in **Table 2**.

Table 2. Estimation of Sugar, Chlorophyll a, Chlorophyll b, Carotenoid, and Proline content of okra plant under induced saline stress and foliar application of TiO_2.

Parameter	**T0**		**T0**		**T1**		**T1**		**T2**		**T2**		**T3**		**T3**	
Verities	**V1**		**V2**		**V1**		**V2**		**V1**		**V2**		**V1**		**V2**	
	reps	**mean**	**reps**	**mean**	**reps**	**mean**	**reps**	**mean**	**reps**	**mean**	**reps**	**mean**	**reps**	**mean**	**reps**	**mean**
Sugar (mg g^{-1})	90.64, 84.48, 89.76	88.29	97.85, 91.2, 96.9	95.32	80.34, 74.88, 79.56	78.26	87.55, 81.6, 86.7	85.28	123.6, 115.2, 122.4	120.4	139.05, 129.6, 137.7	135.45	115.88, 108.0, 114.75	112.88	128.75, 120.0, 127.5	125.42
Chlorophyll a (mg mL^{-1})	0.227, 0.211, 0.224	0.221	0.258, 0.24, 0.255	0.251	2.16, 2.02, 2.14	2.11	2.37, 2.21, 2.35	2.31	2.99, 2.78, 2.96	2.91	3.19, 2.98, 3.16	3.11	2.41, 2.25, 2.39	2.35	2.45, 2.28, 2.43	2.39
Chlorophyll b (mg mL^{-1})	0.978, 0.912, 0.969	0.953	1.08, 1.01, 1.07	1.05	1.17, 1.09, 1.16	1.14	1.29, 1.2, 1.27	1.25	1.75, 1.63, 1.73	1.7	2.01, 1.87, 1.99	1.96	1.24, 1.15, 1.22	1.2	1.49, 1.39, 1.48	1.45
Total carotenoids (mg mL^{-1})	1.18, 1.1, 1.17	1.15	1.34, 1.25, 1.33	1.31	3.4, 3.17, 3.37	3.31	3.71, 3.46, 3.67	3.61	4.79, 4.46, 4.74	4.66	5.25, 4.9, 5.2	5.12	3.91, 3.65, 3.88	3.81	4.89, 4.56, 4.84	4.76
Total Chlorophyll (mg g^{-1})	9.89, 9.22, 9.79	9.63	11.12, 10.37, 11.02	10.84	8.76, 8.16, 8.67	8.53	9.79, 9.12, 9.69	9.53	15.35, 14.3, 15.2	14.95	19.05, 17.76, 18.87	18.56	28.12, 26.21, 27.85	27.39	30.9, 28.8, 30.6	30.1
Proline (µg g^{-1})	22.66, 21.12, 22.44	22.07	24.72, 23.04, 24.48	24.08	31.93, 29.76, 31.62	31.1	36.05, 33.6, 35.7	35.12	82.4, 76.8, 81.6	80.27	97.85, 91.2, 96.9	95.32	58.71, 54.72, 58.14	57.19	72.1, 67.2, 71.4	70.23

3.3.1. Chlorophyll a (mg/g)

In both okra varieties (*Sabaz Pari* and *Savanta*), chlorophyll a was measured at the vegetative stage under saline stress with TiO_2 NP foliar sprays. The highest chlorophyll levels were recorded in T2 and T3, while T1 showed lower values. This indicates that TiO_2 application supports the maintenance of chlorophyll a under stress conditions.

3.3.2. Chlorophyll b (mg/g)

For chlorophyll b, no clear difference was observed between T0 and T1. However, both varieties showed noticeable improvement in T2 and T3, with T3 recording the maximum value. These findings suggest that TiO_2-NPs sprays aid in sustaining chlorophyll b even under salinity stress.

3.3.3. Total chlorophyll (mg/g)

Total chlorophyll content increased in both *Sabaz Pari* and *Savanta* under T2 and T3, whereas T0 and T1 remained at similar levels. These results highlight the overall positive impact of TiO_2-NPs spray on chlorophyll accumulation during stress.

3.4. Carotenoids (mg/g)

Carotenoid levels in both varieties also improved under T2 and T3 compared with other treatments **Table 2**. This suggests that TiO_2-NPs sprays not only enhance chlorophyll but also increase carotenoid content, thereby supporting plant tolerance to stress.

3.5. Osmolytes

To better understand stress responses, osmolytes such as proline and soluble sugars were also analyzed, as they are key markers of tolerance mechanisms in plants. The osmolytes results are depicted in **Table 2**.

3.5.1. Proline (µg/g)

Both okra varieties accumulated higher proline levels in T0 and T1, whereas levels declined in T2 and T3. This reduction suggests that TiO_2-NPs foliar application alleviated stress, thereby reducing the need for high proline accumulation.

3.5.2. Soluble sugars (µg/g)

Soluble sugar content varied significantly across treatments. Clear differences were observed among T0, T1, T2, and T3, indicating that TiO_2-NPs foliar application influenced sugar metabolism under salinity stress.

3.6. Statistical analysis

Two-way ANOVA revealed significant effects of treatment on all measured parameters, including sugar content, chlorophyll a (ChlA), chlorophyll b (ChlB), carotenoids (Carot), total chlorophyll (TChl), and proline ($p < 0.001$; **Table 3**). Variety also significantly influenced all measured traits, although the magnitude of the effect varied among parameters. The interaction between variety and treatment was significant for ChlB, Carot, TChl, and proline, indicating that treatment responses differed between varieties. In contrast, the interaction effect was not significant for sugar content and ChlA, suggesting a consistent treatment response across varieties for these traits. Post-hoc comparison using Tukey's HSD test demonstrated significant differences among treatments for all evaluated parameters (**Table 4**). For sugar content, ChlA, ChlB, and proline, treatment T2 produced the highest mean values, followed by T3, T0, and T1. For carotenoids and total chlorophyll, treatment T3 resulted in the highest values, whereas T0 and T1 generally produced the lowest responses. The grouping of treatments based on Tukey's HSD test confirmed distinct treatment effects, with treatments assigned different significance letters where statistically significant differences occurred ($p \leq 0.05$). Overall, the results indicate that treatment application substantially improved physiological and biochemical traits compared with the control, with T2 and T3 generally producing the most favorable responses across the measured parameters. All the statistical analysis details are provided in the supplementary files.

Table 3. Results of two-way analysis of variance (ANOVA) evaluating the effects of variety, treatment, and their interaction on sugar content, chlorophyll a (ChlA), chlorophyll b (ChlB), carotenoids (Carot), total chlorophyll (TChl), and proline. F-values and corresponding significance levels (*p*-values) are presented for each source of variation.

Parameter	Variety *F*	Variety *p*	Treatment *F*	Treatment *p*	Interaction *F*	Interaction *p*
Sugar	39.876	<0.001	176.559	<0.001	1.503	0.252
ChlA	11.951	0.003	1239.957	<0.001	2.039	0.149
ChlB	39.876	<0.001	272.407	<0.001	3.834	0.030
Carot	64.619	<0.001	1238.148	<0.001	22.537	<0.001
TChl	58.890	<0.001	1057.893	<0.001	5.027	0.012
Proline	90.816	<0.001	1086.967	<0.001	13.093	<0.001

Table 4. Mean responses of sugar content, chlorophyll a (ChlA), chlorophyll b (ChlB), carotenoids (Carot), total chlorophyll (TChl), and proline under different treatments. Different lowercase letters within a parameter indicate significant differences among treatments according to Tukey's honestly significant difference (HSD) test at $p \leq 0.05$.

Parameter	T0	T1	T2	T3
Sugar	c	d	a	b
ChlA	d	c	a	b
ChlB	d	c	a	b
Carot	c	c	b	a
TChl	c	d	b	a
Proline	d	c	a	b

4. Discussion

The FE-SEM analysis illustrated that the prepared TiO_2-NPs possesses relatively uniform, quasi-spherical morphology with slight agglomeration. The histogram (**Figure 1c**) exhibited that the maximum number of particles was dispersed within the range of 50–77 nm, thus, depicting a relatively narrow size distribution. The average particle size was found to be 67.5 nm. The agglomeration may be due to the high surface energy and interparticle attraction among the TiO_2-NPs, which is commonly observed in nanostructured metal oxides due to their high surface energy that promotes strong interparticle interactions. Such agglomeration is a typical characteristic of sol–gel method synthesized TiO_2-NPs [21].

The diffraction peaks appear at 2θ values of 25.36°, 36.95°, 37.81°, 38.57°, 48.09 °, 53.97 °, 55.21 °, 62.71 °, 68.75 °, 70.30 °, 75.10 °, and 82.68 °, can be indexed to the (101), (103), (004), (112), (200), (105), (211), (204), (116), (220), (215), and (224) planes, respectively [22,23]. The crystalline phase of the synthesized TiO_2-NPs was identified by matching the XRD diffraction peaks with standard JCPDS data. The observed diffraction peaks tally well with JCPDS Card No. 21-1272, corresponding to the anatase phase of TiO_2. The observed reflections at 2θ values corresponding to main planes (101), (004), (200), (105), (211), and others confirmed the formation of highly crystalline anatase TiO_2 phase. No impurity peaks associated with rutile or brookite phases were detected, thus showing the high phase purity of the synthesized TiO_2-NPs

[23,24]. The average crystallite size of the as-prepared TiO_2-NPs was calculated using the Scherrer equation, and was typically found in the range of 15–25 nm. However, the particle size obtained from FE-SEM was larger than the crystallite size estimated from XRD analysis. This variance appears because XRD determines the size of single crystalline domains, although FE-SEM measures the size of complete NPs or their clustered structures. Therefore, a single particle observed in FE-SEM may comprise numerous smaller crystallites combined, leading to a comparatively larger particle size. The calculated crystallite size (15–25 nm) from XRD data is consistent with reported values for anatase nanostructures prepared by a sol–gel method [25,26].

Furthermore, the Raman spectroscopic analysis also confirmed that the prepared TiO_2-NPs exist in the anatase phase, with the Eg mode at ~144 cm^{-1} serving as a fingerprint for high-quality anatase phase, as widely reported in the literature [27–29]. The absence of vibrational modes corresponding to rutile or brookite in the Raman spectrum of as-prepared TiO_2-NPs supports the XRD findings. Similar Raman signatures of anatase TiO_2-NPs were reported by many researchers [30,31]. The strong intensity of the Eg peak reflects low defect density and high phase purity, which are essential for photocatalytic efficiency.

EDX analysis confirmed the elemental composition of the synthesized TiO_2-NPs without detectable impurities, in agreement with previous reports on sol–gel derived TiO_2-NPs [24]. In addition to these elements, a minor peak consistent with carbon was also observed. This observed carbon peak in the EDX spectrum may be attributed to the conductive carbon tape used during sample preparation and/or to surface contamination caused by adsorbed atmospheric hydrocarbons present in the dust [32].

Salinity is a key abiotic stress that restrains seed germination, plant growth, and overall productivity in crops, including okra [33]. In the present work, salinity significantly reduced the growth performance of okra (*Abelmoschus esculentus*). This reduction is primarily linked with osmotic stress and ionic toxicity, which mess up water uptake, metabolic activity, and cellular growth progressions. In our study, this was evidently revealed by a substantial decrease in plant height, fresh and dry biomass, and root length under salt stress (**Table 1**). Salinity stress also triggered a noticeable decline in photosynthetic pigments in okra. The decrease in chlorophyll and carotenoids may be due to sodium-induced disruption of chloroplast and pigment biosynthesis. Meanwhile, carotenoids play an important role in defending photosynthetic machinery against oxidative damage; their reduction additionally strengthens stress sensitivity in the plants [34,35]. Consistently, in our experiment, plants with NaCl exhibited a clear reduction in chlorophyll a, chlorophyll b, and total carotenoids (**Table 2**), proving weakened photosynthetic efficiency under stress circumstances.

In the present study, foliar application of as-prepared TiO_2-NPs substantially mitigated the adverse effects of salt stress. Treated plants exhibited enhanced chlorophyll content, good physiological performance, and improved accumulation of osmolytes such as soluble sugars and proline. These compounds subsidize membrane stability, osmotic adjustment, and protection of cellular proteins under stressful circumstances. In our results, TiO_2-NPs-treated okra plants under saline stress displayed higher root and shoot length, as well as increased leaf area, dry and total weight (**Table 1)**. Similarly, the treated plants also showed significantly higher

chlorophyll content, amplified proline buildup, and improved soluble sugar levels compared to untreated stressed plants (**Table 2**), demonstrating effective stress alleviation. These findings are consistent with previous literature on okra, reporting that TiO_2-NPs improve physiological and biochemical performance in stress environments. For instance, the combined use of sewage sludge and TiO_2-NPs enhanced yield and antioxidant activity in okra, although decreasing heavy metal uptake [36]. Likewise, nano-TiO_2 fertilizer exposure altered oxidative responses and stress enzymes in okra [37]. In addition, the incorporation of nano-urea, TiO_2-NPs, significantly improved the growth and yield qualities of okra under field conditions [38].

The enhancements observed under TiO_2-NPs foliar application can be elucidated through multiple mechanisms reported in the relevant literature. TiO_2-NPs boost light absorption efficiency, help electron transport in chloroplasts, and amend nitrogen metabolism. These modifications collectively sustain photosynthetic efficiency under stress situations. Additionally, TiO_2-NPs intensify antioxidant defense systems, thus reducing ROS buildup and restraining lipid peroxidation [39–41]. In addition, salinity-induced oxidative damage is primarily characterized by higher malondialdehyde levels and membrane destabilization. However, TiO_2-NPs application alleviates these adverse effects by strengthening enzymatic and non-enzymatic antioxidant systems. By this means, TiO_2-NPs protect cellular structures and maintain metabolic homeostasis [42–47].

5. Conclusion

Homogeneously dispersed quasi-spherical TiO_2-NPs with anatase phase crystallinity were successfully produced using the sol-gel method, as confirmed by XRD, Raman spectroscopy, EDX, and FE-SEM analyses. Salinity stress poses a major constraint to okra growth during the vegetative stage, where it markedly disrupts physiological functions and inhibits overall development. Evidence from the present study suggests that these detrimental effects can be mitigated through the foliar application of TiO_2-NPs, with the benefits being particularly pronounced in sensitive varieties. The varieties under investigation demonstrated distinct patterns of response to salinity, which can largely be attributed to modifications in their biochemical and physiological processes. The application of TiO_2-NPs appeared to enhance these processes by promoting improved tolerance mechanisms, ultimately supporting better growth and performance under saline conditions. In this study, the TiO_2-NPs as nano-fertilizers suggest their noteworthy potential in improving nutrient uptake and salinity tolerance in okra plants. Thus, the incorporation of TiO_2-NPs into a sustainable agricultural system may offer an effective approach for enhancing okra productivity and resistance under salty environments.

Authors contributions: All authors contributed equally.

Conflicts of interest: The authors declare no conflict of interest.

Data availability: Data is contained in the article.

Reference

1. Javed R, Ain NU, Gul A, et al. Diverse biotechnological applications of multifunctional titanium dioxide nanoparticles: An up-to-date review. IET Nanobiotechnol. 2022;16(5):171–189. doi:10.1049/nbt2.12085
2. Li G, Fang K, Ou Y, et al. Surface study of the reconstructed anatase TiO_2 (001) surface. Prog Nat Sci Mater Int. 2021;31(1):1–13. doi:10.1016/j.pnsc.2020.11.002
3. Baig N, Kammakakam I, Falath W. Nanomaterials: a review of synthesis methods, properties, recent progress, and challenges. Mater Adv. 2021;2(6):1821–1871. doi:10.1039/D0MA00807A
4. Gai X, Xu X, Jiang N, et al. TiO_2 nanomaterial promotes plant growth and disease resistance. Plant Signal Behav. 2025;20(1):2512943. doi:10.1080/15592324.2025.2512943
5. Wang Y, Pei Y, Wang X, et al. Antimicrobial metabolites produced by the plant growth-promoting rhizobacteria (PGPR): Bacillus and Pseudomonas. Adv Agrochem. 2024;3(3):206–221. doi:10.1016/j.aac.2024.07.007
6. Babaei MJ, Ebrahimi A, Heidari P, et al. Titanium dioxide -mediated regulation of enzymatic and non-enzymatic antioxidants, pigments, and diosgenin content promotes cold stress tolerance in Trigonella foenum-graecum L. Sci Rep. 2025;15(1):1837. doi:10.1038/s41598-024-84472-3
7. Bhatti A, Sanchez-Martinez A, Sanchez-Ante G, et al. Synergistic Effect of TiO_2-Nanoparticles and Plant Growth-Promoting Microorganisms on the Physiological Parameters and Antioxidant Responses of Capsicum annum Cultivars. Antioxidants. 2025;14(6):707. doi:10.3390/antiox14060707
8. Delaix CL, Tomiozzo A, Weber G, et al. Interplay among hormones, antioxidants, and redox signaling in abiotic stress responses. Environ Exp Bot. 2025;229:106081. doi:10.1016/j.envexpbot.2024.106081
9. Islam W, Sanaullah T, Khalid N, et al. Plants, Environmental Constraints, and Climate Change. In: Fahad S, ed. Climate Change and Plants. 1st ed. Boca Raton, FL: CRC Press; 2021:171–192. doi:10.1201/9781003108931-13-13
10. Ullah F, Ali S, Siraj M, et al. Plant Microbiomes Alleviate Abiotic Stress-Associated Damage in Crops and Enhance Climate-Resilient Agriculture. Plants. 2025;14(12):1890. doi:10.3390/plants14121890
11. Khan NA, Owens L, Nuñez MA, et al. Complexity of combined abiotic stresses to crop plants. Plant Stress. 2025;17:100926. doi:10.1016/j.stress.2025.100926
12. De Souza Junior JP, Kadyampakeni DM, Shahid MA, et al. Mitigating abiotic stress in citrus: the role of silicon for enhanced productivity and quality. Plant Stress. 2025;16:100837. doi:10.1016/j.stress.2025.100837
13. Mwesige FF. The extent and distribution of salt-affected soils in sub-Saharan Africa from 1970 to the present: a review of the current state of knowledge. Front Soil Sci. 2025;5:1571243. doi:10.3389/fsoil.2025.1571243
14. Khan N. Decoding phytohormone signaling in plant stress physiology: Insights, challenges, and future directions. Environ Exp Bot. 2025;231:106099. doi:10.1016/j.envexpbot.2025.106099
15. Muhammad M, Waheed A, Wahab A, et al. Soil salinity and drought tolerance: An evaluation of plant growth, productivity, microbial diversity, and amelioration strategies. Plant Stress. 2024;11:100319. doi:10.1016/j.stress.2023.100319
16. Demo AH, Gemeda MK, Abdo DR, et al. Impact of soil salinity, sodicity, and irrigation water salinity on crop production and coping mechanism in areas of dryland farming. Agrosyst Geosci Environ. 2025;8(1):e70072. doi:10.1002/agg2.70072
17. Rehman SU, Yang J, Zhang J, et al. Salt stress in wheat: A physiological and genetic perspective. Plant Stress. 2025;16:100832. doi:10.1016/j.stress.2025.100832
18. Sorapong B. Okra (*Abelmoschus esculentus* (L.) Moench) as a valuable vegetable of the world. Ratar Povrt. 2012;49(1):105–112. doi:10.5937/ratpov49-1172
19. DuBois M, Gilles KA, Hamilton JK, et al. Colorimetric Method for Determination of Sugars and Related Substances. Anal Chem. 1956;28(3):350–356. doi:10.1021/ac60111a017
20. Zou M, Yuan L, Zhu S, et al. Effects of heat stress on photosynthetic characteristics and chloroplast ultrastructure of a heat-sensitive and heat-tolerant cultivar of wucai (*Brassica campestris* L.). Acta Physiol Plant. 2017;39(1):30. doi:10.1007/s11738-016-2319-z
21. Ahmad MM, Mushtaq S, Al Qahtani HS, et al. Investigation of TiO_2 Nanoparticles Synthesized by Sol-Gel Method for Effectual Photodegradation, Oxidation and Reduction Reaction. Crystals. 2021;11(12):1456. doi:10.3390/cryst11121456
22. Abdul Razaq AA, Jasim FH, Chiad SS, et al. Effect of annealing temperature on the physical of nanostructured TiO_2 films prepared by sol-gel method. J Optoelectron Res. 2024;20(2):131–141. doi:10.15251/JOR.2024.202.131

23. Li T, Abdelhaleem A, Chu W, et al. S-doped TiO_2 photocatalyst for visible LED mediated oxone activation: Kinetics and mechanism study for the photocatalytic degradation of pyrimethanil fungicide. Chem Eng J. 2021;411:128450. doi:10.1016/j.cej.2021.128450
24. Khan JA, Han C, Shah NS, et al. Ultraviolet–Visible Light–Sensitive High Surface Area Phosphorous-Fluorine–Co-Doped TiO_2 Nanoparticles for the Degradation of Atrazine in Water. Environ Eng Sci. 2014;31(7):435–446. doi:10.1089/ees.2013.0486
25. Preda S, Pandele-Cușu J, Petrescu SV, et al. Photocatalytic and Antibacterial Properties of Doped TiO_2 Nanopowders Synthesized by Sol−Gel Method. Gels. 2022;8(10):673. doi:10.3390/gels8100673
26. Zhang Y, Wan J, Ke Y. A novel approach of preparing TiO_2 films at low temperature and its application in photocatalytic degradation of methyl orange. J Hazard Mater. 2010;177(1–3):750–754. doi:10.1016/j.jhazmat.2009.12.095
27. Bayati MR, Moshfegh AZ, Golestani-Fard F. On the photocatalytic activity of the sulfur doped titania nano-porous films derived via micro-arc oxidation. Appl Catal A Gen. 2010;389(1–2):60–67. doi:10.1016/j.apcata.2010.09.003
28. Huang H, Yan H, Duan M, et al. TiO_2 surface oxygen vacancy passivation towards mitigated interfacial lattice distortion and efficient perovskite solar cell. Appl Surf Sci. 2021;544:148583. doi:10.1016/j.apsusc.2020.148583
29. Kalampaliki T, Makri SP, Papadaki E, et al. Visible-Light Active Sulfur-Doped Titania Nanoparticles Immobilized on a Silica Matrix: Synthesis, Characterization and Photocatalytic Degradation of Pollutants. Nanomaterials. 2021;11(10):2543. doi:10.3390/nano11102543
30. Buono C, Desimone M, Schipani F, et al. N-doping effects on the oxygen sensing of TiO_2 films. J Electroceram. 2018;40(1):72–77. doi:10.1007/s10832-017-0100-3
31. El-Deen SS, Hashem AM, Abdel Ghany AE, et al. Anatase TiO_2 nanoparticles for lithium-ion batteries. Ionics. 2018;24(10):2925–2934. doi:10.1007/s11581-017-2425-y
32. Marycleopha M, Yaou Balarabe B, Adjama I, et al. Anhydrous sol-gel synthesis of TiO_2 nanoparticles: Evaluating their impact on protein interactions in biological systems. J Trace Elem Miner. 2024;7:100114. doi:10.1016/j.jtemin.2023.100114
33. Atta K, Mondal S, Gorai S, et al. Impacts of salinity stress on crop plants: improving salt tolerance through genetic and molecular dissection. Front Plant Sci. 2023;14:1241736. doi:10.3389/fpls.2023.1241736
34. Stefanov MA, Rashkov GD, Yotsova EK, et al. Impact of Salinity on the Energy Transfer between Pigment–Protein Complexes in Photosynthetic Apparatus, Functions of the Oxygen-Evolving Complex and Photochemical Activities of Photosystem II and Photosystem I in Two Paulownia Lines. Int J Mol Sci. 2023;24(4):3108. doi:10.3390/ijms24043108
35. Shumaila K, Chandni Z, Tayyaba R, et al. The significance of chlorophylls and carotenoids in enhancing seed tolerance to abiotic stress. Biol Clin Sci Res J. 2024;2024(1). doi:10.54112/bcsrj.v2024i1.1065
36. Kumar P, Alamri SAM, Alrumman SA, et al. Foliar use of TiO_2-nanoparticles for okra (*Abelmoschus esculentus* L. Moench) cultivation on sewage sludge–amended soils: biochemical response and heavy metal accumulation. Environ Sci Pollut Res. 2022;29(44):66507–66518. doi:10.1007/s11356-022-20526-1
37. Ogunkunle CO, Adegboye EF, Okoro HK, et al. Effect of nanosized anatase TiO_2 on germination, stress defense enzymes, and fruit nutritional quality of *Abelmoschus esculentus* (L.) Moench (okra). Arab J Geosci. 2020;13(3):120. doi:10.1007/s12517-020-5121-6
38. Razauddin, Maji S, Kumar S, et al. Use of nano fertilizers to reduce chemical fertilizer load for okra production. Plant Arch. 2025;25(1). doi:10.51470/PLANTARCHIVES.2025.v25.no.1.182
39. Mehta D, Vyas S. Comparative bio-accumulation of osmoprotectants in saline stress tolerating plants: A review. Plant Stress. 2023;9:100177. doi:10.1016/j.stress.2023.100177
40. Haghpanah M, Hashemipetroudi S, Arzani A, et al. Drought Tolerance in Plants: Physiological and Molecular Responses. Plants. 2024;13(21):2962. doi:10.3390/plants13212962
41. Kaur G, Sanwal SK, Kumar A, et al. Role of osmolytes dynamics in plant metabolism to cope with salinity induced osmotic stress. Discov Agric. 2024;2(1):59. doi:10.1007/s44279-024-00070-x
42. Methela NJ, Islam MS, Das AK, et al. Antioxidant mechanisms in salt-stressed Maize (Zea mays L.) seedlings: comparative analysis of tolerant and susceptible genotypes. Appl Biol Chem. 2024;67(1):109. doi:10.1186/s13765-024-00963-x
43. Ayala A, Muñoz MF, Argüelles S. Lipid Peroxidation: Production, Metabolism, and Signaling Mechanisms of Malondialdehyde and 4-Hydroxy-2-Nonenal. Oxid Med Cell Longev. 2014;2014:1–31. doi:10.1155/2014/360438
44. Zahra M, Abrahamse H, George BP. Flavonoids: Antioxidant Powerhouses and Their Role in Nanomedicine. Antioxidants. 2024;13(8):922. doi:10.3390/antiox13080922

45. Gonz áez-Ocampo HA, Mart ínez-Álvarez IG, Jaramillo-Flores ME, et al. Comparison of Phenolic and Flavonoid Content and Antioxidant and Chelating Activities of Rhizophora mangle in Different Anthropogenically-Polluted Coastal Lagoons. Front Mar Sci. 2022;9:791748. doi:10.3389/fmars.2022.791748
46. Goncharuk EA, Zagoskina NV. Heavy Metals, Their Phytotoxicity, and the Role of Phenolic Antioxidants in Plant Stress Responses with Focus on Cadmium: Review. Molecules. 2023;28(9):3921. doi:10.3390/molecules28093921
47. Dilnawaz F, Misra AN, Apostolova E. Involvement of nanoparticles in mitigating plant's abiotic stress. Plant Stress. 2023;10:100280. doi:10.1016/j.stress.2023.100280